NeuroImage 227 (2021) 117613

Contents lists available at ScienceDirect

NeuroImage

journal homepage: www.elsevier.com/locate/neuroimage

# Brain plasticity dynamics during tactile Braille learning in sighted subjects: Multi-contrast MRI approach

Jacek Matuszewski[a,*], Bartosz Kossowski[a], Łukasz Bola[a,b], Anna Banaszkiewicz[a], Małgorzata Paplińska[c], Lucien Gyger[d], Ferath Kherif[d], Marcin Szwed[b], Richard S. Frackowiak[e], Katarzyna Jednoróg[f], Bogdan Draganski[d,g], Artur Marchewka[a,*]

[a] Laboratory of Brain Imaging, Nencki Institute of Experimental Biology, Polish Academy of Sciences, Warsaw, Poland
[b] Institute of Psychology, Jagiellonian University, Krakow, Poland
[c] Maria Grzegorzewska University, Warsaw, Poland
[d] LREN, Department for Clinical Neurosciences, CHUV, University of Lausanne, Lausanne, Switzerland
[e] École Polytechnique Fédérale de Lausanne, Lausanne, Switzerland
[f] Laboratory of Language Neurobiology, Nencki Institute of Experimental Biology, Polish Academy of Sciences, Warsaw, Poland
[g] Department of Neurology, Max Planck Institute for Human Cognitive and Brain Sciences, Leipzig, Germany

ARTICLE INFO

*Keywords:*
Brain plasticity
Longitudinal design
Tactile Braille reading
Intracortical myelin
Multimodal MRI
Quantitative MRI

ABSTRACT

A growing body of empirical evidence supports the notion of diverse neurobiological processes underlying learning-induced plasticity changes in the human brain. There are still open questions about how brain plasticity depends on cognitive task complexity, how it supports interactions between brain systems and with what temporal and spatial trajectory. We investigated brain and behavioural changes in sighted adults during 8-months training of tactile Braille reading whilst monitoring brain structure and function at 5 different time points. We adopted a novel multivariate approach that includes behavioural data and specific MRI protocols sensitive to tissue properties to assess local functional and structural and myelin changes over time. Our results show that while the reading network, located in the ventral occipitotemporal cortex, rapidly adapts to tactile input, sensory areas show changes in grey matter volume and intra-cortical myelin at different times. This approach has allowed us to examine and describe neuroplastic mechanisms underlying complex cognitive systems and their (sensory) inputs and (motor) outputs differentially, at a mesoscopic level.

## 1. Introduction

Over the last decades neuroimaging studies have shown that adult brains are capable of functional and structural reorganization during new skill acquisition. This phenomenon is known as experience-dependent neuroplasticity and is widely studied in human and animal models. Such studies have proposed various neurobiological mechanisms, involving among others dendritic branching and synaptogenesis, axon sprouting, glial changes or myelin remodelling (Zatorre et al., 2012). Newly gained skills, if complex, may require novel motor, sensory and higher cognitive functional configurations that might, in turn, modulate the process of brain reorganization at a mesoscopic level. Learning that induces changes beyond the trained function, may result in cross-modal plasticity (Cecchetti et al., 2016). However, most scientific evidence comes from studies of the impact on motor or sensory skill acquisition, whilst plastic changes resulting from associated changes in cognitive abilities remain to be investigated (Wenger et al., 2017).

Over 15 years ago, the first longitudinal studies showed that information derived from T1-weighted (Draganski et al. 2004) and diffusion-weighted images (Bengtsson et al., 2005) can be used to trace structural plasticity during new skill acquisition. However, relationships between brain activity and anatomical changes are also often overlooked, notably because most studies involve only 2 time points (before and after training), which provides a crude appreciation of the temporal dynamics of regional tissue reorganization. Furthermore, non-quantitative imaging is generally difficult to interpret because signal changes may be driven by multiple coordinated structural changes of various tissue types (for review see Zatorre et al., 2012; Tardif et al. 2016; Lerch et al. 2017).

Recent advances in multi-parameter MRI techniques quantifying brain tissue properties offer a newer approach to characterisation of the relationship between brain microstructure, function and behaviour (Draganski et al. 2011; Weiskopf et al. 2015; Tardif et al. 2016). Based on human and animal studies it has been proposed that myelin may play an important role in the process of neuroplasticity by fine-tuning

* Corresponding authors.
*E-mail addresses:* j.matuszewski@nencki.edu.pl (J. Matuszewski), a.marchewka@nencki.edu.pl (A. Marchewka).

https://doi.org/10.1016/j.neuroimage.2020.117613
Received 16 June 2020; Received in revised form 20 November 2020; Accepted 29 November 2020
Available online 8 December 2020

information processing (Fields, 2015; Heath et al., 2017; Kaller et al., 2017; Sampaio-Baptista and Johansen-Berg, 2017). Myeloarchitectural reorganization has been seen in white (Hofstetter et al., 2013; Sampaio-Baptista et al., 2013; Scholz et al., 2009) and grey matter (Draganski et al. 2011; Grydeland et al. 2013; Carey et al. 2018a). Further, myelin plasticity, not synaptic pruning, is important in producing cortical thinning of the ventral occipitotemporal cortex (vOTC) during development (Natu et al., 2019).

One technique sensitive to intracortical myelination is quantitative T1 mapping, which has been shown to reflect grey matter myeloarchitecture (Bock et al., 2009; Lutti et al., 2014; Sereno et al., 2013; Stüber et al., 2014). Recently, the method has been used to segregate the written-language sensitive part of the vOTC - the visual word form area (VWFA; Dehaene and Cohen 2011; Price and Devlin 2011) - into lexical and perceptual components (Lerma-Usabiaga et al., 2018). As detailed relationships between brain function and structural tissue properties during complex learning are still lacking (Lövdén et al., 2013; Tardif et al., 2016; Zatorre et al., 2012), we decided to use a cognitively intense sensorimotor task to examine the distribution and dynamics of neuroplasticity associated with learning to read by touch. We used Braille as a model for three reasons: (1) it is a sensory-motor skill related to language and thus, engages both simple perceptive and higher-order cognitive processing; (2) it offers insight into cross modal plasticity as it recruits the early visual cortex and the vOTC of blind (Büchel et al., 1998; Reich et al., 2011; Sadato et al., 1996) and trained sighted subjects (Bola et al., 2019; Merabet et al., 2008; Siuda-Krzywicka et al., 2016); (3) the results from previous studies using a similar paradigm with 2 time points (before - after) showed functional (Siuda-Krzywicka et al., 2016) and structural reorganization in visual (Bola et al. 2017) and somatosensory (Debowska et al., 2016) cortex, allowing us to formulate prior predictions regarding the localisation of plastic changes.

A group of twenty-six sighted subjects completed an 8-month tactile Braille reading course and were enrolled into behavioural and multicontrast MRI sessions at 5 time points (TP). This allowed us to trace the time courses of functional and structural brain reorganization. Given the nature of tactile reading and results from previous studies, we hypothesized neuroplastic reorganization in the early somatosensory cortex, early visual cortex and the reading network of the vOTC and left inferior frontal gyrus (Broca's area). In this setup, Braille is a novel sensory input processed in a functioning language network, so we hypothesized that functional changes related to reading should occur early, followed in time by increases in tactile reading speed and structural changes (GMV and intracortical myelination) associated with optimization of tactile input processing in somatosensory and visual cortices.

## 2. Material and methods

### 2.1. Subjects

Thirty-two sighted, right-handed females (age mean, M = 23.2 years; standard deviation, SD = 3.3) took part in tactile Braille reading course and MRI sessions. Six of them were excluded due to anatomical abnormalities (2 subjects) or dropping out (4 subjects). Thus, 26 (age M = 23.1; SD = 3.4) were included in the analyses. All were native Polish speakers and had normal or corrected to normal vision and were naïve to the Braille alphabet. Twenty-two of them were students or postgraduates of studies in special education for the blind, 3 were working in a charitable foundation helping blind people and one was working part-time as a Braille visual transcriber. Participants were familiar with the basics of visual Braille but naïve to tactile reading (see: Results, section 3.1). Informed consent and MRI safety screenings were collected prior to the study. The study was approved by the Committee for Research Ethics of the Institute of Psychology of the Jagiellonian University. All subjects were new and had not participated in previous studies regarding brain plasticity previously published by members of our research group (Bola et al., 2016, 2017b, 2017a; Siuda-Krzywicka et al., 2016), however 21 of them participated in a recently published transcranial magnetic stimulation study (Bola et al., 2019).

### 2.2. Experimental design

Over the course of tactile reading training participants underwent 5 behavioural testing and brain imaging sessions approximately 2.5 months apart: pre-exposure (Time Point 0; TP0), two during (TP1, TP2) and one at the end of training (TP3). There was a final follow-up imaging study 2.5 months after the end of training (TP4, see Fig 1A). MRI sessions included acquiring functional images measuring brain responses to tactile Braille reading and structural anatomical images as well as quantitative T1 mapping. Subjects received financial gratification both for participation in the Braille course and for each of the MRI sessions.

### 2.3. Tactile reading course and performance tests

The tactile reading course lasted 8 months and involved meetings with an instructor and self-paced work with sets of 30 exercise cards per month. Meetings with the instructor were organized for the whole group 2 times per month in the first 2 months and in smaller groups (5–10 subjects) once per month subsequently. Self-paced work was based on 30 cards given monthly with each card representing around 15–20 min of tactile reading, resulting in approximately 20–25 h of instruction between each TP. Subjects were instructed to read as regularly as possible. Due to the demanding nature of the tactile reading process, the course covered only 16 Polish Braille letters (A, B, C, D, E, I, K, L, Ł, M, O, P, S, T, U, Y). The first 10 h or so of training involved basic principles of hand movements as well as basic shape discrimination and then letters and words were introduced, starting with easier ones (A, B, C, D, E, I, K, O) while the more difficult ones (L, Ł, M, S, P, T, U, Y) were taught 3 months into training (Fig 1A). Details of the tactile Braille course for sighted subjects were described in Bola et al. (2016). During the first three months of tactile training 13 subjects reported a preference for reading with the left-hand despite being right-handed. This phenomenon was reported previously both in blind and sighted subjects (Sadato et al., 2002; Siuda-Krzywicka et al., 2016), however since tactile reading involves using both hands simultaneously (with one hand supporting navigation between words and lines and the other one reading), actual tactile input is similar for both fingers.

The tactile reading test consisted of 20 Braille words (3–5 letters long) with SUBTLEX-PL (Mandera et al., 2014) frequency occurrence over 1 per million. The task was to read aloud as many words as they could within 60 s with their preferred hand, while blindfolded. Only words read correctly were counted. Twelve different versions of the test were used, counterbalanced across subjects and matched for word length and letters introduced during the course. Additionally, subjects were tested in tactile single letters reading and performing visual Braille reading (see sup. materials 1.1 for details).

### 2.4. MRI protocols

MRI data were acquired using Siemens Trio 3T scanner with a 12-channel coil. Structural T1-weighted (T1w) image was acquired with a standard MPRAGE sequence with the following parameters: FOV: 256 × 256 mm, voxel size: 1 × 1 × 1 mm, TR: 2530 ms, TE: 3.32 ms, FA: 7°, 176 slices. T1-maps were acquired via Variable Flip Angle method(Preibisch and Deichmann, 2009) with 3D gradient-echo, 1mm-isotropic resolution scans with FA = 4° and FA = 18° (TE = 2.46 ms, TR = 7.6 ms, TA = 2*5 min 27 s). Maps were corrected for flip angle error by B1+ map (stimulated echo to spin echo ratio). Functional data were acquired using an echo planar imaging pulse sequence with the following parameters: field of view: 216 × 216 mm, isometric voxel

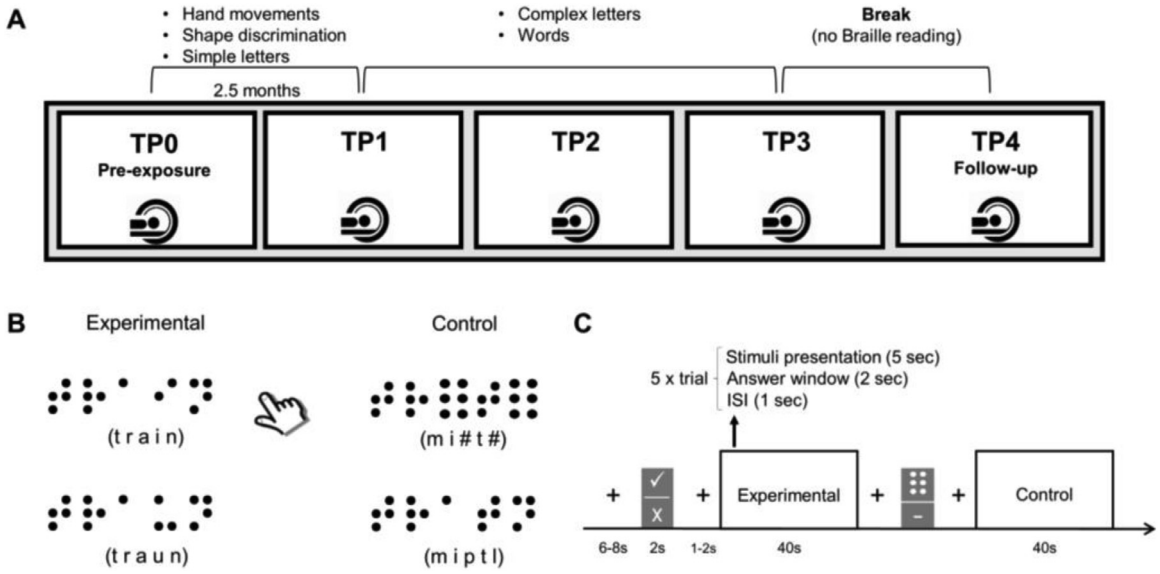


**Fig. 1.** Experimental design and fMRI task overview. A. Subjects trained in tactile Braille reading for 8 months and participated in 5 MRI and behavioural testing sessions performed 2.5 months apart. TP = Time Point. B. During fMRI sessions subjects performed lexical decision tasks tactually via a dedicated Braille display (Debowska et al., 2013). In the experimental condition participants had to discriminate real words (left upper panel) from pseudo-words (left lower panel). In the control condition they had to indicate whether there were 2 full Braille characters present among consonant strings (right upper panel) or not (right lower panel). C. Stimuli were presented in a block design with jittered inter-block intervals and cues indicating the task in between. Each block consisted of 5 stimuli. ISI = inter-stimulus interval.

size: 3 mm, matrix 72 × 72, TR: 2500 ms, TE: 28 ms, flip angle: 80°, 41 slices in the AC–PC plane with an odd interleaved order.

### 2.5. fMRI task and stimuli

During each TP, the LDT was performed with tactile reading. After brief instruction subjects were presented with alternating experimental and control blocks. During the experimental condition they had to decide whether a presented stimulus constituted a word or a pseudoword. In the control condition they had to decide whether 2 target symbols (full six-dot Braille characters) were present amongst consonant strings (see Fig 1B and C for design overview and example stimuli). Before each block, a fixation cross was presented for 6–8 s, followed by 2 s of a visual cue alerting subjects to the type of following block (experimental or control), and another fixation cross (1–2 s). Blocks consisted of 5 stimuli presented for 5 s each. Each stimulus within a block was followed by a 2 s response time and a 1 s inter-stimulus interval. Each block lasted 40 s and there were 8 blocks in each tactile condition (12 min 50 s in total).

Words used in LDTs were taken from the SUBTLEX-PL linguistic database (Mandera et al., 2014), with several restrictions: (1) they had to be 3- to 5-letters long; and (2) they had an occurrence frequency higher than 1 per million. Pseudowords for LDTs were created by changing one letter within a word in a way that makes the resulting string orthographically and phonologically plausible but, at the same time, not meaningful in Polish. Tactile words and pseudowords were formed only from letters used during Braille training. Control stimuli were created by substituting vowels in words and pseudowords with consonants known to subjects. Additionally, 2 letters were pseudo-randomly replaced with target symbols in half the trials (i.e. k#dm#, ##pt, see Fig 1B for examples).

Stimulus sets in TPs were matched to the material covered during the course (i.e. all letters in words were known to participants at the time of testing, except for TP0). Additionally, they were matched in word length, frequency and neighbour size. Stimuli used in TP0 and TP4 were identical, as the subjects were naïve to tactile reading before training. Subjects were not blindfolded during tactile reading and no instructions were given regarding whether they should keep their eyes closed or open. Tactile stimuli were presented via an MRI-compatible Braille display (Debowska et al., 2013) and visual stimuli were presented on a screen. Subjects gave answers by response pads held in the non-reading hand.

In addition, in order to test the specificity of functional reorganization to tactile reading, a visual version of the LDT (involving reading in the Latin alphabet and a visual perceptual control task) were also performed during each TP. Details of these procedures and analyses are described in Supplementary Information 1.3. Data from visual and tactile LDTs obtained in TP3 were additionally used as functional localizers in our recent study using transcranial magnetic stimulation (Bola et al., 2019).

### 2.6. Image processing

T1w images used in voxel based morphometry (VBM) were preprocessed with SPM12 (Wellcome Trust Centre for Human Neuroimaging, http://www.fil.ion.ucl.ac.uk/spm) software running on MATLAB 2016b (Mathworks, http://www.mathworks.com). First, for each subject, images from five time points were registered and bias-corrected using the serial longitudinal registration (Ashburner and Ridgway, 2013) implemented in SPM12. This method avoids potential TP asymmetry biases by using spatially warped, intensity-corrected versions of mid-point average T1w (avgT1) scan. Average images were classified into tissue classes using the enhanced tissue probability maps for optimal delineation of subcortical structures (Lorio et al., 2016) followed by the diffeomorphic registration DARTEL approach (Ashburner, 2007) that uses a study-specific template. Grey matter probability maps from the previous step were multiplied by Jacobian determinants to obtain time-point specific, bias-corrected maps of volume deformation between the particular time-point and the mid-point average data. The product image was subsequently registered to standard MNI space using the DARTEL registration parameters and smoothed with an 8 mm full-width-at-half-maximum (FWHM) isotropic Gaussian kernel. Functional images from all TPs were realigned to the first scan and motion corrected, resulting in 6 head movement parameters (describing translation and rotation in X,

Y and Z axes) for each image in each TP, used in the statistical analyses. Next, the mean functional image was co-registered to subject's avgT1 image, normalized to MNI space via its deformation field and smoothed with a 6 mm FWHM Gaussian kernel.

T1-maps were first reconstructed from Proton density-weighted and T1w images with in-house MATLAB routines following Helms et al. (2008), including B1 and spoiling corrections (Preibisch and Deichmann, 2009). The obtained maps were then co-registered to and multiplied by combined grey matter, white matter and cerebrospinal fluid masks from a segmented avgT1 to rule out numerical noise created by image division (Preibisch and Deichmann, 2009). Next, T1 maps were spatially registered to MNI space using the registration parameters obtained from the T1w data and finally smoothed using the weighted-averaging strategy (Draganski et al., 2011) implemented in the hMRI-Toolbox (Tabelow et al., 2019) with 8 mm Gaussian FWHM. Given that T1 relaxation time has a negative relationship to myelination, we calculated longitudinal relaxation rate (R1 = 1/T1) to uniform directionality of changes over time between methods (Lutti et al., 2014).

### 2.7. Statistical analyses

Behavioural data were analysed with repeated measures analysis of variance (rmANOVAs): one-way with time (5) as factor and two way with time (5) and condition (2) as factors for tactile reading speed and LDT performance respectively). Due to incomplete data (resulting from technical issues with response pads) LDT results are reported for 21 subjects. Post-hoc tests were computed with Bonferroni correction for multiple comparisons. Greenhouse-Geisser F-tests and degrees of freedom corrections were used for cases with a violated sphericity assumption.

Functional data were first analysed in a general linear model (GLM) at the subject level. Timings of experimental and control blocks and visual cues were entered into separate, TP-specific design matrices with addition of six head movement regressors of no interest. Hemodynamic response was modelled with a box-car function built into SPM12. Data were filtered with a 128 Hz high-pass filter. Then, *experimental* > *control* contrasts were computed for each subject at each TP.

In order to provide common resolution for multivariate analysis of variance (MANOVA) data analysis between modalities, all pre-processed images (or subject-level contrasts for fMRI) were resliced to a unified voxel size (Mcfarquhar et al., 2016) (2 × 2 × 2 mm) and z-scored at the voxel level within each given modality (based on means and SDs from all subjects in all TP for fMRI, R1 and GMV respectively). Additionally, to ensure optimal space for all analyses and avoid issues with absolute thresholds, the SPM Masking Toolbox (Ridgway et al., 2009) with SPM8 was used to compute masks for model estimation. Specifically, 3 masks were created based on sequence-specific data and then multiplied by each other resulting in an optimally-thresholded mask containing only voxels present in all data.

A MANOVA model was specified via the Multivariate SPM (MSPM) toolbox (https://github.com/LREN-CHUV/MSPM) as a multivariate extension of univariate GLM (Chen et al., 2014; Mcfarquhar et al., 2016). Data from all modalities were used to create a

$$Y = XB + E$$

model where Y is a matrix of all observations (subject x TP) divided into separate modalities (fMRI, R1, GMV) and X is the design matrix with *time* (TP0-TP4) and *subject* factors, B is the matrix of model parameters and E is the matrix of errors (Fox, 2015). Since a MANOVA design consists of two design matrices – in this case, one addressing MRI modalities and the other time effects - multimodal training effects were analysed by a combination of two contrasts. We used a combination of identity matrix F tests with all modalities (also known as an *L* contrast) and a pre-(TP0) vs end of training (TP3) comparison for the time condition (known as a *c* contrast). These contrasts were thresholded at the voxel level with Family Wise Error (FWE) multiple comparisons correction ($p < 0.05$) with a cluster extent of 20 voxels. An anatomical mask was subsequently used in unimodal analyses.

To explore multimodal effects, all neuroimaging data were analysed in modality-specific 5 × 1 rmANOVA designs with time (TP0-TP4) as a factor. An additional *subject* factor was also added to account for dependency of the acquired data. Pairwise comparisons between TPs were performed to explore the effects of Braille training within each modality. These contrasts were then masked with results from relevant MANOVA contrasts and thresholded at the voxel level with FWE multiple comparisons correction ($p < 0.05$) and a cluster extent of 20 voxels. Since all of the comparisons were performed within subjects, confounding factors like variability in age, total intracranial volume, Braille reading skills were controlled on a subject level and thus were not included in the design matrices. Independent brain regions used in detailed analyses were obtained from cytoarchitectonic maps calculated in Anatomy toolbox (Eickhoff et al., 2005). In order to assure high spatial precision all anatomical maps were thresholded with at least 20% probability of being classified as a given structure. Somatosensory regions of interest (ROIs) were defined by combination of Brodmann areas 3a and 3b, early visual cortices by combining V1 and V2. Broca's area was defined as a combination of left Brodmann areas 44 and 45 (left Inferior Frontal Gyrus, IFG). The lexically-specific vOTC ROI was defined as an 8mm radius sphere (MNI X -41.54, Y -57.67 and Z -10.18) according to Lerma-Usabiaga et al. (2018). All ROIs were analysed with 3 (MRI modality: fMRI, R1, GMV) x 5 (Time: TP0 – TP4) rmANOVAs with Greenhouse-Geisser non-sphericity corrections and Bonferroni-corrected post hoc tests.

Finally, we calculated repeated-measures correlations between tactile Braille reading speed (measured with words per minute) and functional and structural tissue properties. Analyses were performed with the *rmcorr* package (Bakdash and Marusich, 2017) in R 3.4.3 (R Core Team, 2020). This approach allows to use all repeated measures' data points for common while not violating the assumption of observations' independence by using analysis of covariance to adjust for inter-individual variability. Thus, this method estimates a common slope based on the changes over time in both of the correlated measures. Specifically, correlations were performed between behavioural results from tactile Braille words reading speed and all MRI contrasts (fMRI, R1, GMV) extracted from the above-mentioned ROIs (namely: Broca's area, lexically-specific vOTC and bilateral early somatosensory and visual cortices). Each correlation was computed by using 2 measures of interest (behavioural score and contrast-and-ROI-specific z-scored extracted values) and a "participant" factor adjusting the repeated measures nature of the data. Obtained p values were multiplied by 18 (3 MRI contrasts x 6 ROIs) in order to correct them for multiple comparisons.

Statistical analyses were performed in GraphPad Prism 8.3 software (GraphPad Software, La Jolla California, USA). Error bars on plots were adjusted to correctly reflect the variance in the within-subject design (see Cousineau, 2005 for details).

## 3. Results

### 3.1. Behavioural results

Participants knew the basis of visual Braille reading but were naïve to tactile reading. Prior to training 1 of 26 subjects was able to read 3 words, one subject read 2 words and 2 subjects read 1 word per minute (group M = 0.31; SD = 0.11, range 0–3). Subjects were also able to read a few tactile letters and visual Braille words (TP0 letters M = 8.27; SD = 1.14, range 2–18; TP0 visual words M = 10.54; SD = 0.22, range 0–22, see supplementary materials 1.1 for details). At the end of training subjects were able to read around 8 words per minute (M = 8.04; SD = 4.13, range 1–17). The ANOVA showed a significant effect of time ($F_{(4,96)} = 60.73$; $p < 0.0001$) indicating reading improvement. Post-hoc tests between adjacent TP pairs showed significant increases in reading

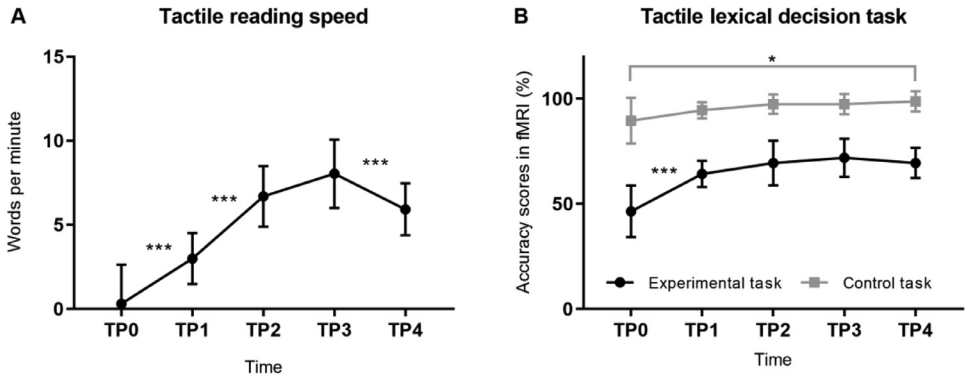


**Fig. 2.** Behavioural performance during tactile reading training. A Tactile Braille word reading speed during training. B Tactile Lexical Decision Task (black) and Control task (tactile symbol detection, grey) performance during MRI (see: Methods). Error bars represent standard deviations adjusted for within-subject designs (Cousineau, 2005). TP = time point, $^{*}p < 0.05$, $^{***}$ $p < 0.001$, Bonferroni corrected.

speed between TP0 and TP1 ($t_{(26)} = 7.2$, $p_{corr} < 0.0001$), TP1 and TP2 ($t_{(26)} = 6.4$, $p_{corr} < 0.0001$) as well as significant decrease at follow up (TP4) compared to the last training (TP3) test ($t_{(26)} = 4.8$, $p_{corr} < 0.001$) (Fig 2A).

Behavioural performance in the tactile Lexical Decision Task (LDT) administered during MRI was at chance level at TP0 (M = 46.5 %; SD = 9.4, $t_{(20)} = 1.7$, $p = 0.101$) confirming subject naïveté to tactile Braille and an inability to distinguish words from pseudo-words (see Fig 2B for details). After training an average accuracy of 71.9 % (SD = 20.3) was achieved. The basic tactile control discrimination was relatively easy with average scores ranging from 89.6% (TP0; SD = 14.2) to 98.8 % (TP4; SD = 2.7). A two-way repeated measures (rm)ANOVA revealed a significant main effect of time ($F_{(4,80)} = 29.2$, $p < 0.0001$), condition ($F_{(1,20)} = 132.2$, $p < 0.0001$) and a time x condition interaction ($F_{(4,80)} = 5.6$, $p = 0.0005$). Post hoc comparisons within conditions showed significant improvement for the experimental condition between TP0 and all other TPs ($ps_{corr} < 0.0001$) and improvement with the control condition between TP0 and TP4 ($p_{corr} = 0.022$).

### 3.2. Braille training effects: whole brain analyses

First, we created a multivariate analysis of variance (MANOVA) model by pooling imaging data from all time-points (TP0-TP4) and modalities (fMRI, R1, GMV) and combining their respective data vectors into a unified design matrix (see Materials and Methods for details). Results from the contrast measuring cumulative effects of training (TP3 vs TP0) indicated that tactile reading acquisition invoked neuronal reorganization in bilateral visual, motor, premotor and somatosensory cortices, left fusiform gyrus, as well as bilateral superior, middle and inferior frontal gyri and the left lingual gyrus (Fig 3A). Coordinates and anatomical labels of all peaks are presented in Table 1. Next, similar contrasts in unimodal within-subject ANOVAs were performed to disentangle the modality-specific contributions to these effects.

Follow-up unimodal analysis of brain activation during tactile Braille reading (*experimental* > *control*) revealed increased activity after training (TP3 > TP0) in a large network involving bilateral motor and somatosensory cortex, left vOTC (with peak MNI coordinates X = -44, Y = -58 and Z = -6), inferior frontal gyri, both thalami, superior parietal cortices and cerebellum (Fig 3B, upper panel). The inverted contrast (TP0 > TP3) indicated relatively reduced involvement of both angular gyri, precuneus and inferior temporal gyri. Coordinates and anatomical labels of all peaks are presented in Table 2. Additionally, we tested the specificity of these changes to tactile reading by comparisons of activity changes in the visual (Latin alphabet) version of the LDT (see Supplementary Information 1.3).

In terms of structural (myelin-associated) reorganization, R1 increases were found in right superior and both middle frontal gyri and in left vOT cortex (with peak MNI coordinates X = -46, Y = -50 and Z = -10) partially overlapping with a functionally delineated cluster (Fig 3B, middle panel, see also Supplementary Information FigS10). Detailed information about MNI coordinates and anatomical labels is located in Table 3. Voxel-based morphometry analysis showed increased relative GMV in the sensory regions including right early visual cortex, right pre- and postcentral gyrus as well as bilateral cuneus and superior occipital gyri (Fig 3B, lower panel). Anatomical labels and MNI coordinates for GMV statistical map peaks are presented in Table 4. There were no significant decreases in R1 or GMV between TP0 and TP3. Detailed whole-brain comparisons between all TPs can be found in supplementary materials (1.2).

**Table 1**
Significant differences between TP0 and TP3 explained by linear combination of all studied MRI modalities (fMRI, R1, GMV) in the repeated measures MANOVA model. Anatomical structures were labelled with Anatomy Toolbox atlas. X, Y and Z are MNI coordinates. Up to 3 peaks with minimal 15 mm distance are reported per cluster.

| Region Label | Extent | F-value | X | Y | Z |
|---|---|---|---|---|---|
| L Precentral Gyrus | 19510 | 42.8 | -52 | 0 | 40 |
| Location not in atlas | 19510 | 39.2 | -22 | -4 | 50 |
| R Precentral Gyrus | 19510 | 38.0 | 44 | -2 | 32 |
| L Angular Gyrus | 1879 | 40.5 | -48 | -60 | 40 |
| R Cerebellum (VI) | 2261 | 37.0 | 26 | -56 | -24 |
| Location not in atlas | 2261 | 25.4 | -22 | -54 | -24 |
| Cerebellar Vermis (9) | 2261 | 24.4 | 4 | -58 | -24 |
| L Fusiform Gyrus | 450 | 30.6 | -42 | -56 | -8 |
| R Angular Gyrus | 1394 | 29.6 | 54 | -58 | 30 |
| R Insula Lobe | 494 | 23.4 | 34 | 20 | 2 |
| L Middle Frontal Gyrus | 707 | 20.1 | -38 | 26 | 48 |
| L Middle Frontal Gyrus | 707 | 16.2 | -22 | 38 | 40 |
| Location not in atlas | 50 | 19.4 | 6 | -26 | -6 |
| R Superior Frontal Gyrus | 126 | 18.6 | 22 | 22 | 62 |
| L Inferior Temporal Gyrus | 160 | 18.2 | -64 | -28 | -12 |
| L Middle Temporal Gyrus | 56 | 17.4 | -62 | -42 | -4 |
| R Middle Frontal Gyrus | 972 | 17.4 | 40 | 44 | 8 |
| R Superior Frontal Gyrus | 972 | 16.4 | 16 | 50 | 44 |
| R IFG (p. Triangularis) | 972 | 14.5 | 46 | 32 | 30 |
| R Inferior Temporal Gyrus | 99 | 17.1 | 54 | -60 | -10 |
| R Superior Medial Gyrus | 79 | 16.5 | 4 | 56 | 6 |
| Location not in atlas | 94 | 16.3 | -10 | 16 | 32 |
| L Superior Orbital Gyrus | 102 | 15.3 | -22 | 54 | 2 |
| Location not in atlas | 24 | 13.8 | -34 | -42 | -6 |
| L Superior Temporal Gyrus | 68 | 13.8 | -54 | -38 | 22 |
| L Inferior Temporal Gyrus | 21 | 13.6 | -54 | -18 | -26 |
| R Superior Medial Gyrus | 45 | 13.4 | 8 | 62 | 24 |
| R Inferior Temporal Gyrus | 24 | 13.0 | 54 | -4 | -28 |
| L Lingual Gyrus | 53 | 12.1 | 0 | -72 | 10 |
| L Middle Frontal Gyrus | 43 | 11.8 | -22 | 50 | 24 |
| L Mid Orbital Gyrus | 32 | 11.7 | -4 | 52 | 0 |

### 3.3. Detailed brain reorganization time courses

Having confirmed the general anatomical and functional patterns of brain reorganization during training how to read Braille, we performed an anatomically-instructed approach to investigate detailed time courses

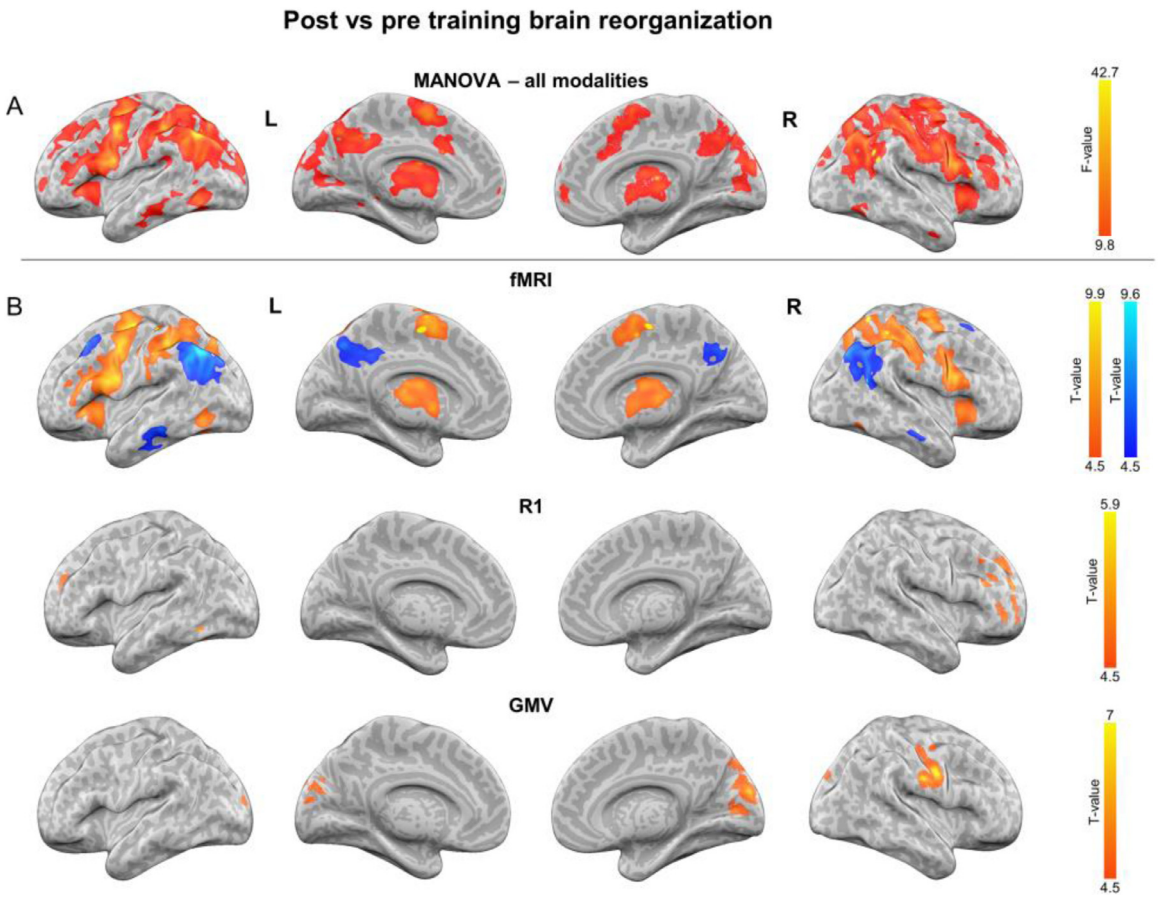


**Fig. 3.** Post (TP3) - vs pre-training (TP0) brain reorganization. A. Multivariate analysis of variance (MANOVA) results. Results show differences between TP0 and TP3 in all of the measured MRI modalities. B. Unimodal follow-up test. Upper panel: fMRI results of *experimental* > *control* contrast in the tactile lexical detection task. Middle panel: longitudinal relaxation rate (R1) results indicative of intracortical myelin changes. Lower panel: voxel-based morphometry indicating relative grey matter volume (GMV) increases. For unimodal analysis red-yellow colour maps indicate increases (post- > pre-training; TP3 > TP0) and blue-cyan colour maps indicate decreases (pre- > Post-training; TP0 > TP3). All maps are thresholded at $p < 0.05$, FWE (Family-Wise Error) corrected at the voxel level with an additional cluster extent threshold of 20 voxels. L = left hemisphere, R = right hemisphere.

and interactions between tissue properties. For this purpose, we used an independent cytoarchitectonic atlas (Eickhoff et al., 2005) to create masks of Broca's area and early somatosensory and visual cortices. Additionally, the lexically-sensitive part of vOTC was defined based on recent literature (Lerma-Usabiaga et al., 2018). Data were extracted from subject reading-specific fMRI contrasts, R1 and GMV at all TPs (see Methods for details). The main focus of this analysis was a comparison of temporal dynamics of structural and functional reorganization, by testing for interactions between time (TP0 – TP4) and modality (fMRI, R1, GMV).

Significant time x modality interactions were found in both language processing structures, Broca's area and lexical vOTC ($F_{(5, 123.8)} = 8.9$, $p < 0.0001$ and $F_{(4.5, 112.6)} = 3.9$, $p = 0.004$, respectively). Both showed similar patterns of changes during tactile Braille based lexical processing compared to non-lexical control tasks. Pairwise comparisons corrected across all time points and modalities showed significant functional differences between TP0 and all other TPs for Broca's area (all $ps_{orr} = 0.003$) and lexical vOTC (TP1 > TP0 $p_{corr} = 0.012$; TP2 > TP0 $p_{corr} = 0.018$; TP3 > TP0 $p_{corr} = 0.003$; TP4 > TP0 $p_{corr} = 0.003$). This pattern of changes was specific to tactile reading and was not due to task repetition (Supplementary Information 1.3). Additionally, post-hoc tests for lexical vOTC showed an R1 increase between TP0 and TP3 ($p_{corr} = 0.015$). There were no significant GMV changes over time, Fig 4A and B.

Next, a similar approach was used to examine primary sensory areas, namely bilateral early somatosensory and visual cortices. Data from all TPs and modalities revealed significant time x modality interactions for left ($F_{(5.3, 132)} = 2.6$, $p < 0.025$) and right ($F_{(5, 125.7)} = 7.4$, $p < 0.0001$) early somatosensory cortices, indicating differences in reorganization time courses between MRI measures. Pairwise comparisons for the left somatosensory cortex showed linear increases in brain activation between TP0 and TP3 ($p_{corr} = 0.009$). There were no significant differences in R1 values between TPs. VBM results showed a tendency to a linear increase of GMV between TP0 and TP4 ($p_{corr} = 0.024$) and TP1 and TP4 ($p_{corr} = 0.033$), even in the follow up scan, Fig 5A. In early right somatosensory cortex (Fig 5B) functional responses were higher in all TPs than in TP0 (TP1 > TP0 $p_{corr} < 0.003$; TP2 > TP0 $p_{corr} = 0.009$; TP3 > TP0 $p_{corr} < 0.003$; TP4 > TP0 $p_{corr} < 0.003$). Additionally, a GMV increase was observed between TP0 and TP3 ($p_{corr} = 0.048$) and TP4 ($p_{corr} = 0.009$) as well as TP1 and TP4 ($p_{corr} < 0.003$). No significant effects were observed for R1.

Identical interaction analysis performed for early visual cortex did not reach significance in left ($F_{(5.1, 126.8)} = 1$, $p = 0.417$) or right ($F_{(4.3, 108)} = 0.7$, $p = 0.583$) hemispheres. However, we found significant GMV increases over time (see Fig 5C and D and Supplementary Information 1.5 for details). We did not observe any functional response changes to reading in the early visual cortex. While many studies have demonstrated the role of this region in the detailed spatial processing of tactile stimuli (Bola et al., 2019; Saito et al., 2006; Zangaladze et al., 1999), responses to language processing (which was targeted by our contrast) were found previously only in congenitally blind subjects (Bedny et al., 2011; Burton et al., 2003) but not in sighted subjects learning Braille (Debowska et al. 2016; Siuda-Krzywicka et al. 2016).

**Table 2**
Local maxima from follow-up unimodal contrasts between pre-(TP0) and post-training (TP3). fMRI represents brain activation changes in the tactile LDT (*experimental* > *control*). Anatomical structures were labelled with the Anatomy toolbox atlas. X, Y and Z are MNI coordinates. Up to 3 peaks with minimal 15 mm distance are reported per cluster.

| Modality (contrast) | Region Label | Extent | t-value | X | Y | Z |
|---|---|---|---|---|---|---|
| fMRI (TP3 > TP0) | R Cerebellum (VI) | 1109 | 9.9 | 26 | -58 | -26 |
| | Location not in atlas | 1109 | 7.9 | 4 | -58 | -22 |
| | L Superior Frontal Gyrus | 3191 | 9.4 | -22 | -4 | 52 |
| | L Precentral Gyrus | 3191 | 9.4 | -54 | 2 | 40 |
| | L IFG (p. Opercularis) | 3191 | 8.8 | -46 | 2 | 20 |
| | L Inferior Parietal Lobule | 1955 | 8.8 | -38 | -36 | 44 |
| | L Inferior Parietal Lobule | 1955 | 7.7 | -34 | -50 | 58 |
| | L Superior Parietal Lobule | 1955 | 7.2 | -18 | -68 | 46 |
| | L Posterior-Medial Frontal | 639 | 8.8 | 0 | 2 | 60 |
| | R Superior Frontal Gyrus | 600 | 8.6 | 26 | -10 | 60 |
| | R IFG (p. Opercularis) | 891 | 8.6 | 50 | 8 | 20 |
| | R Precentral Gyrus | 891 | 7.1 | 52 | 4 | 40 |
| | R Postcentral Gyrus | 1896 | 8.4 | 54 | -20 | 52 |
| | Location not in atlas | 1896 | 8.0 | 34 | -36 | 40 |
| | R Postcentral Gyrus | 1896 | 7.1 | 44 | -36 | 62 |
| | L Thalamus | 1676 | 8.3 | -10 | -18 | 10 |
| | Location not in atlas | 1676 | 7.6 | -8 | 4 | 2 |
| | R Thalamus | 1676 | 7.6 | 10 | -16 | 6 |
| | Location not in atlas | 616 | 8.0 | -22 | -54 | -24 |
| | L Inferior Temporal Gyrus | 281 | 7.8 | -44 | -58 | -6 |
| | R Insula Lobe | 260 | 6.9 | 32 | 18 | 2 |
| | R Inferior Temporal Gyrus | 22 | 5.5 | 52 | -56 | -10 |
| fMRI (TP0 > TP3) | L Angular Gyrus | 1251 | 9.6 | -50 | -58 | 40 |
| | R Angular Gyrus | 981 | 7.5 | 44 | -68 | 40 |
| | R Middle Temporal Gyrus | 981 | 6.7 | 48 | -52 | 20 |
| | L Precuneus | 637 | 7.2 | 0 | -62 | 42 |
| | Location not in atlas | 637 | 6.3 | -10 | -44 | 36 |
| | L Middle Frontal Gyrus | 201 | 7.0 | -40 | 24 | 48 |
| | L Inferior Temporal Gyrus | 116 | 7.0 | -64 | -28 | -12 |
| | R Superior Frontal Gyrus | 32 | 5.9 | 22 | 22 | 62 |
| R1 (TP3 > TP0) | R Superior Frontal Gyrus | 177 | 5.5 | 26 | 42 | 20 |
| | L Inferior Temporal Gyrus | 30 | 5.3 | -46 | -50 | -10 |
| | R IFG (p. Triangularis) | 28 | 4.9 | 46 | 32 | 30 |
| R1 (TP0 > TP3) | - | - | - | - | - | - |
| GMV (TP3 > TP0) | R Precentral Gyrus | 407 | 7.0 | 52 | -6 | 30 |
| | R Calcarine Gyrus | 480 | 6.4 | 6 | -82 | 20 |
| | L Cuneus | 68 | 5.3 | -14 | -84 | 20 |
| | R Superior Occipital Gyrus | 29 | 4.9 | 22 | -76 | 40 |
| GMV (TP0 > TP3) | - | - | - | - | - | - |

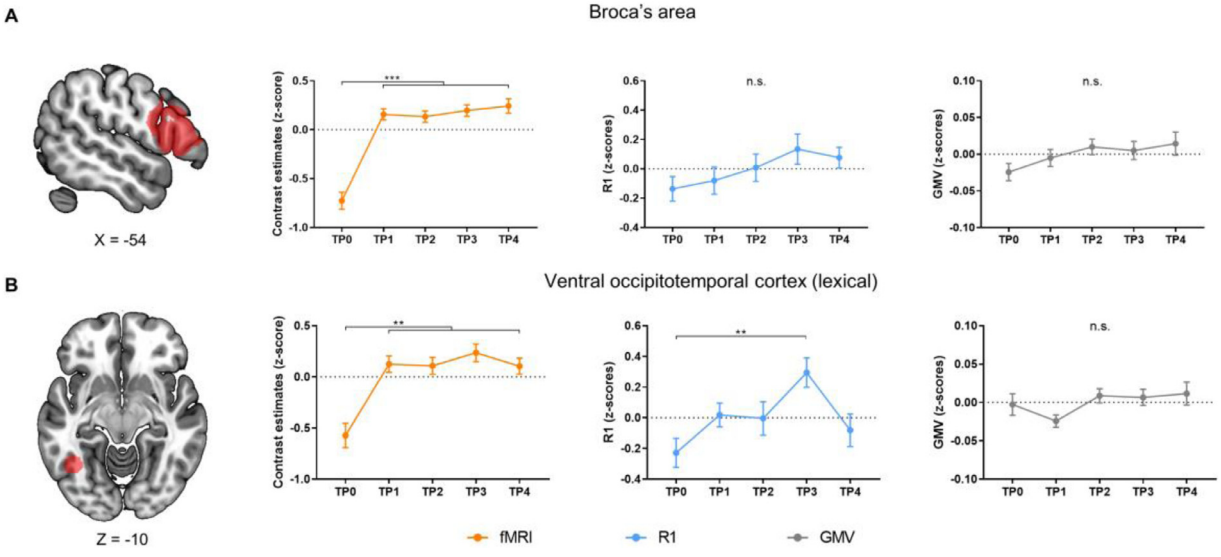


**Fig. 4.** Time course of functional and structural brain reorganization during tactile reading training in Broca's area (A) and the lexically-sensitive part of vOTC (Lerma-Usabiaga et al., 2018) (B). fMRI represents *experimental* > *control* contrast in tactile LDT. TP = Time Point, n.s. = no significant effect of time, $^{**}p < 0.01$, $^{***}p < 0.001$, Bonferroni corrected for all TPs and modalities. Error bars represent standard errors of the mean, adjusted for within-subject design(Cousineau, 2005).

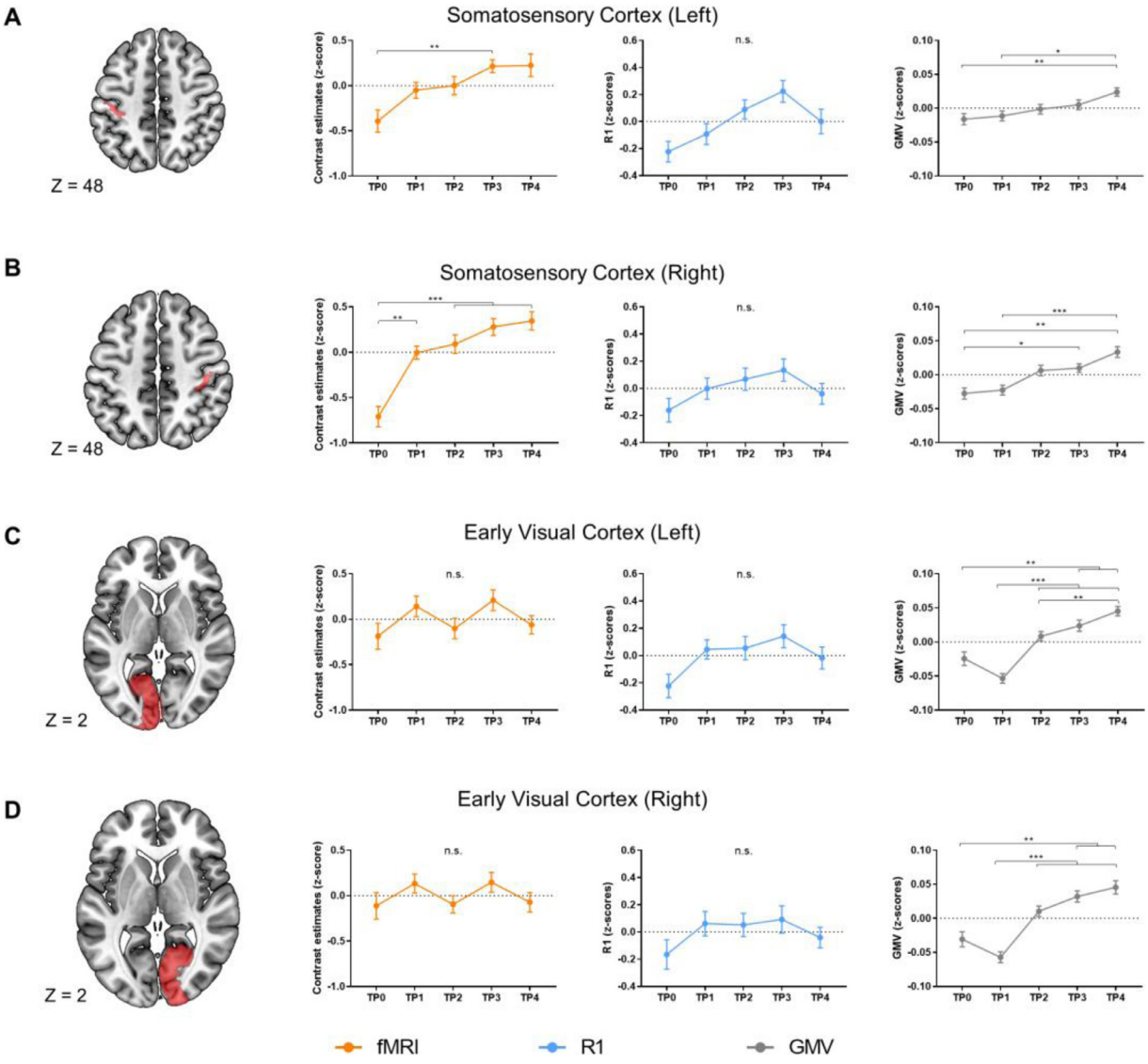


**Fig. 5.** Time course of functional and structural brain reorganization during tactile reading training in the early sensory regions: left (A) and right (B) somatosensory cortex and left (C) and right (D) early visual cortex. fMRI represents *experimental* > *control* contrast in tactile LDT. TP = Time Point, n.s. = not significant effect of time, $^{*}p < 0.05$, $^{**}p < 0.01$, $^{***}p < 0.001$, Bonferroni corrected for all TPs and modalities. Error bars represent standard error of the mean, adjusted for within-subject design (Cousineau, 2005).

These results suggest that during Braille acquisition, functional reorganization in the reading network occurs rapidly and further optimisation is reflected in increased intracortical myelination in vOTC. On the other hand, changes observed in the somatosensory cortex supporting basic tactile input evaluation and early visual cortex which takes part in detailed spatial analysis (Bola et al., 2019; Merabet et al., 2008; Zangaladze et al., 1999) manifest gradually, as the novel experiences and resultant cerebral processing lead to changes in local GMV.

### 3.4. Brain-behaviour correlations

To test the association between functional and structural brain properties with Braille reading skills, we computed repeated measures correlations (Bakdash and Marusich, 2017) between tactile reading speed (measured by words per minute) and z-scored values of fMRI contrast estimates, R1 parameter and GMV at each TP. Correlations showed a significant positive relationship between tactile reading speed and functional brain responses of the Broca's area ($r_{rm(103)} = 0.53$; *pcorr* < 0.001), vOTC ($r_{rm(103)} = 0.44$; *pcorr* < 0.001), left ($r_{rm(103)} = 0.35$; *pcorr* < 0.01) and right ($r_{rm(103)} = 0.52$; *pcorr* < 0.001) early somatosensory cortices. No significant correlations were found in the early visual cortices ($r_{rm(103)} = 0.20$; *pcorr* 0.828; $r_{rm(103)} = 0.15$; *pcorr* > 0.99 for left and right hemisphere accordingly). R1 parameter was significantly correlated with Braille reading skills in the left early somatosensory cortex ($r_{rm(103)} = 0.34$; *pcorr* < 0.01). Positive correlations with R1 were also found in the language processing areas, but they did not survive the correction for multiple comparisons (Broca's $r_{rm(103)} = 0.20$; *puncorr* = 0.046; *pcorr* = 0.828; vOTC $r_{rm(103)} = 0.22$; *puncorr* = 0.026; *pcorr* = 0.468). Significant correlations with the GMV were limited to the sensory areas, namely the right early somatosensory cortex ($r_{rm(103)} = 0.33$; *pcorr* < 0.01) and left ($r_{rm(103)} = 0.39$; *pcorr* < 0.001) and right ($r_{rm(103)} = 0.37$; *pcorr* < 0.001) early visual cortices. Initially significant correlation with GMV of the left somatosensory cortex did not survive the multiple comparisons ($r_{rm(103)} = 0.17$; *puncorr* = 0.007; *pcorr* = 0.126). No relationships were found with the GMV of language-processing areas (Broca's $r_{rm(103)} = 0.04$; *pcorr* > 0.99; vOTC $r_{rm(103)} = 0$; *pcorr* > 0.99). Reported correlation coefficients are summarized in Fig. 6. Scatter plots for each analysis are presented in the Supplementary Infor-

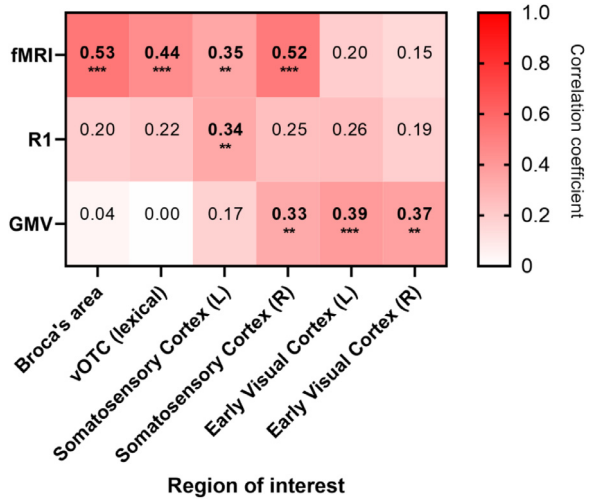


**Fig. 6.** Repeated measures correlation coefficients between brain function and structure and tactile Braille reading speed (words per minute) at all time points. Bolded coefficients reached statistical significance after correction for multiple comparisons. fMRI represents *experimental* > *control* contrasts from tactile lexical decision task; R1 = longitudinal relaxation rate indicative of intramyelin content, GMV = grey matter volume; vOTC = ventral occipitotemporal cortex; L = left; R = right; *** $p < 0.001$; ** $p < 0.01$, Bonferroni corrected for multiple comparisons. Scatterplots for correlations are located in Supplementary Information 1.6.

mation 1.6 (Figures S11-S13). Additionally, similar analyses were performed with the data solely from TP1 and TP3, revealing strong positive correlations between tactile reading speed and the GMV of the early visual cortex ($r_{rm(25)} = 0.71$, pcorr < 0.001 and $r_{rm(25)} = 0.72$, pcorr < 0.001 for left and right hemisphere accordingly). These results are described in Supplementary Information 1.6.

## 4. Discussion

Our longitudinal multi-contrast MRI study provides strong evidence that learning-induced brain plasticity changes are reflected in distinct, brain tissue-specific spatial and temporal patterns (Fig 3). We show the interaction between neural activity and brain anatomy as a function of experience-dependent cross-modal plasticity. As predicted, changes in neural response specific to tactile reading occur during the first stage of training, resulting in activation of the language network, which then remains stable. On the other hand, anatomical reorganization proceeds more gradually with GMV increases limited to the somatosensory and visual cortices. Furthermore, inclusion of a quantitative T1 mapping technique shows R1 increases in lexical vOTC, supporting the role of intra-cortical myelination in the neuroplastic changes of learning. Our results open new avenues for discussion about the relationships between experience-induced brain activity and local structural reorganization.

We demonstrate that tactile reading in sighted subjects can be incorporated into a functioning language network during the first weeks of learning. 76 Our results are consistent with previous studies showing similar effects (Debowska et al., 2016; Siuda-Krzywicka et al., 2016) and expand them by demonstrating an interaction between functional and microstructural properties of the vOTC. In line with our hypotheses, a rapid functional response change is seen during the first part of learning, accompanied by structural changes over the whole course of training, as measured by longitudinal relaxation rate (R1) measurements (Fig 4, also see Supplementary Information Fig S10).

Inclusion of the quantitative MRI technique of T1 mapping revealed structural changes which were not detected in morphometry. Here we show training induced increase in the intra-cortical myelin content in the lexically-sensitive part of the vOTC which is crucial for reading. Moreover, this change overlapped with the brain activity increases. The main function of myelin is to increase the impulse conduction speed along the axon, which results in faster transmission across long distances in the brain (Freeman et al., 2016). Consequently, intra-cortical myelin fine-tunes local neuronal circuits by insulating the axons within the grey matter (Glasser et al., 2014). The mechanism of activity-dependent myelination was recently proposed as important consideration to the learning-induced remodeling on the synapse level (Fields, 2015). While in our data R1 increases in the vOTC were observed between pre- and post-training scan, they were followed by decreases in the follow-up (Fig. 4B) suggesting that myelin may be responsible for neuroplasticity modulation on a fine-tuned temporal scale. Therefore, with a growing body of evidence suggesting that activity-dependent regulation of myelin content plays an important role in learning, this often-overlooked phenomenon may offer a complementary way in which novel experiences shape the brain (Sampaio-Baptista and Johansen-Berg, 2017).

We also demonstrate how complex skill acquisition and its components affect grey matter at different time scales, which brings an interesting perspective to studies investigating neuroplastic change. In previous studies, task-relevant changes induced by various learning protocols were detected in sensory regions following remapping of somatotopy (Kolasinski et al., 2016), somatosensory stimulation (Schmidt-Wilcke et al., 2018), musical training (Herholz and Zatorre, 2012) or new colour naming (Kwok et al., 2011). On the other hand, higher-order association cortices were also reported to reorganize during second language acquisition (Li et al., 2014), Morse-code learning (Schmidt-Wilcke et al., 2010) or memory training (Engvig et al., 2010). However, striking differences in the cellular and myeloarchitectonic components (Glasser et al., 2014) and also in local cortical thickness (Fischl and Dale, 1999) of sensory and associative areas are reported. These factors may have a differential impact on learning-associated mechanisms of plasticity. Our results support this view by displaying distinct spatial and temporal patterns of functional and structural reorganization over the course of learning a novel, cognitively complex skill. Braille reading involves processing of the tactile input in the somatosensory cortex and basic spatial processing of Braille dots and characters in the early visual cortex (Merabet et al., 2008; Saito et al., 2006; Zangaladze et al., 1999). Neuroimaging data from non-human primates and humans indicate that the tactile information is most likely transferred to the visual cortex via cortico-cortical route (with additional thalamo-cortical connections following sensory deprivation, (Müller et al., 2019)). In the macaque brain the shortest route from S1 to V1 involves the S2, ventral intraparietal area, middle temporal visual area, V3 and parieto-occipital cortex (Négyessy et al., 2006). Studies in humans confirm this cortico-cortical connection (Klinge et al., 2010; (Kupers et al., 2006) Ptito et al., 2005; Wittenberg et al., 2004). Therefore, after basic evaluation of the information in the somatosensory cortex, the Braille input would be sent to the early visual cortex specialized in the detailed spatial processing. Next, the tactile input in the visual cortex follows the hierarchy similar to the typical (visual) processing (Bola et al., 2019). In this view, after detailed spatial analysis in the early visual cortex, tactile input is evaluated in the high-level visual areas, responsible for orthographic analysis. This gradient of information flow, from basic sensory and spatial evaluation to abstract linguistic analysis, could possibly occur beyond the vOTC. In line with the reading model proposed by Dehaene (2009), linguistic information would be then distributed across the reading network, including fronto-temporal regions (e.g. inferior frontal gyrus, Amedi et al., 2001, 2007; Siuda-Krzywicka et al., 2016) involved in access to meaning or articulation.

In the course of learning, linking tactile stimuli with letter meaning occurs early (Fig 1A), which activates the language processing areas (Broca's area and vOTC). These behaviourally relevant activations remain stable (Fig 4) despite the absence of GMV changes and gradual behavioural progress in tactile reading speed. This result is interesting from two perspectives. First, this highlights the flexibility of the visuo-

frontal reading network. The involvement of the vOTC in the processing of non-visual modalities has been summarized by various hypotheses (e g. Pattamadilok et al., 2019). While previous hypotheses mostly refer to spoken (auditory modality) and written (visual modality) language processing, they might be true also for tactile reading. Specifically, the tactile reading represents a novel, atypical input into the vOTC, but the underlying cognitive processes resemble the (typical) visual reading, i.e. extraction of letter and word forms from "written" symbols. This view is in line with studies showing vOTC response to tactile reading in blind (Reich et al., 2011) and trained sighted subjects (Siuda-Krzywicka et al., 2016). This flexibility is compatible with the task-specific organization of the brain (Amedi et al., 2017; Pascual-Leone and Hamilton, 2001), suggesting that the vOTC neurons might be specialized in certain computations independently of the sensory modality or multimodal in general. Therefore, such innate organization could be the mechanism explaining this rapid change in response, occuring during the very first weeks of training.

The second perspective is the lack of activity changes in the later time points. We believe that this phenomenon might be explained by the proficiency of our subjects. Specifically, tactile reading is a demanding skill, and even after 8 months of learning participants were able to read around 8 words per minute, which is at the level reached by blind children in the first grade. During learning, the initial mismatch between supply and the demands should lead to expansion of the cortex, followed by a renormalization (Lövdén et al., 2013; Wenger et al., 2017), during which an optimal circuit is chosen. Thus, we should observe an increase in activity followed by a decrease representing optimization and cognitive "effortlessness" in the execution of the trained skill. In our data such differences could be observed in the language areas (Broca's area, vOTC) response to tactile (demanding, not optimized) and visual (effortless, optimized) versions of the lexical decision tasks (Figure S9). A similar rapid activity increase followed by the lack of changes during adult learning was recently reported during the acquisition of sign language (Banaszkiewicz et al., 2020) and Greek language (Kuper et al., 2020). Moreover, during reading acquisition in children the peak of vOTC response to words occurs in the second grade (Brem et al., 2013; Mauer et al., 2007). This activity is then levelled off with more practice from second to fifth grade (Mauer et al., 2011). Mechanistically, this increase could be explained by the interactive account of the vOTC's contribution to reading proposed by Price and Devlin (2011). In this view, the activity increase would be driven by synthesis of bottom-up sensory input (present even at the TP0) and the top-down predictions that are generated automatically from prior experience (only observed from TP1 onwards). Thus, the biggest prediction error and brain activity in vOTC is expected at the initial stages of learning to read. Next, with increased proficiency, this activity would require less cognitive effort, demonstrated by lower contrast estimates over time. Unfortunately, due to the demanding nature of tactile reading, our design was too short to capture that last phase of learning. Therefore, we are not able to observe the functional changes beyond TP1.

We observed a different time course in sensory regions (Fig 5) where the tactile input is evaluated. GMV in the somatosensory and visual cortices seems to follow a supply-demand model (Lövdén et al., 2013) in which the local relative grey matter volume increases until the demands for optimal processing are met. The exact biological mechanisms underlying volumetric changes are still under debate. It is not clear whether VBM changes reflect changes in general brain morphology, tissue microstructure, or a combination of both (Lövdén et al., 2013). Multiple candidate cellular mechanisms have been proposed, including neurogenesis, dendritic branching (synaptogenesis), gliogenesis or axon sprouting (Zatorre et al., 2012). Animal studies showed that training-induced GMV increases correlated with a marker of neuronal remodelling and not neurogenesis or size changes (Lerch et al., 2011). Nevertheless, the T1-weighted contrast is affected by multiple factors, therefore the exact cellular mechanisms explaining volumetric changes are not easy to interpret (Draganski et al., 2014; Lerch et al., 2017; Tardif et al., 2016). The dissociation between sensory and associative areas suggests differential mechanisms governing structural plasticity in the two. In this view, refinement of a novel input in early sensory regions is indexed by GMV, while the lack of R1 changes reflects an adequate initial level of cortical myelination, which is known to be greater in these areas than in associative cortices (Glasser et al., 2014). Neuronal densities are higher in primary visual and somatosensory areas (Collins et al., 2010), which are also characterized by higher myelin content (Glasser and Van Essen, 2011). An inverse relation was found in the lightly myelinated areas. Therefore, myelin content is negatively correlated with intracortical circuit complexity, i.e. more myelin content characterizes simpler and less dynamic intracortical circuits. Thus, one possible explanation for the lack of R1 changes in the sensory cortices is that the higher degree of myelination in those areas may inhibit further cortical plasticity as there is no more "room" for change (Chen et al., 2000; McGee and Strittmatter, 2003; McGee et al., 2005). Instead, these changes might be shifted to optimization of white matter tracts (detected by i.e. fractional anisotropy), which were reported in the sensorimotor and visual cortices following tactile reading training in sighted subjects (Bola et al., 2017b; Debowska et al., 2016). On the other hand, an increase in myelination of higher order visual areas as a mechanism of structural plasticity optimises their functionality. Myelination of the vOTC was previously identified as a marker of increasing functional specialization during development (Gomez et al., 2017). Here, we demonstrate that it might also be an adaptation to training in adults. We support the hypothesis that activity-dependent myelination (Fields, 2015) may be a mechanism contributing to brain plasticity (Sampaio-Baptista and Johansen-Berg, 2017) in the visual cortex specialized for lexical processing.

The brain is shaped by interactions with the environment, which then impact behaviour, cortical activity and various aspects of anatomy (Zatorre et al., 2012). In turn, improvements in behaviour are a product of an interplay between a variety of structural and functional changes (Gomez et al., 2017). In order to build predictions about learning, we considered temporal interactions between many factors contributing to the structural and functional properties of cortices. Here we investigated differences and similarities between structural and functional changes in space and time. While we show that these changes follow distinct time courses with functional changes preceding structural ones, the exact relationship between the two is profoundly complex. Neuroplasticity represents the mismatch between environmental demands (new experiences or acquired skills) and the local supplies (computational capacity of the brain region, Lövdén et al., 2010). Thus, the structural changes observed in the tissue result from the computational mismatch in the tissue. Only after such mismatch is prolonged, the somewhat "sluggish" structural changes occur. Previous studies have shown that the functional and structural changes observed via MRI often do not overlap spatially or temporally (Haier et al., 2009; Ilg et al., 2008; Schmidt-Wilke et al., 2010), as their effects might be driven by independent processes or changes occurring at the network level (Tardif et al., 2016). In our study, functional plasticity preceded the structural changes in the temporal aspect, which is in line with the view that the anatomical changes might be a somewhat slower adaptation to the environmental demands. Spatial convergence between structure and function was observed in the somatosensory cortex, critical to the tactile input evaluation, and vOTC involved in orthographic processing. Interestingly, both functional responses and the volume observed in the early somatosensory cortex was positively correlated with the tactile reading speed. Therefore, while the spatial overlaps may be limited, they occurred in the areas relevant to tactile reading and reflected the learning rate of the participants. In conjunction with the temporal profiles of change, we could speculate that the early functional change "drives" the structural reorganization. These results might hint at different mechanisms underlying functional and structural plasticity operating at the network level.

There are three main limitations to this study. First, although it was shown that myelin concentration makes a major contribution to T1 con-

trast (Stüber et al., 2014), it is also sensitive to tissue iron content (Callaghan et al., 2015; Tardif et al., 2016). However, these relationships may vary across brain regions. Therefore, a weighted approach combining multiple methods sensitive to tissue myelin content would be more optimal in future studies (Heath et al., 2017; Sampaio-Baptista and Johansen-Berg, 2017). Second, while we demonstrate structural plasticity caused by a novel experience, namely learning (GMV increase in the early visual cortex), the exact cellular mechanisms governing this change are still unclear. Multiple tissue properties contribute to the signal from weighted imaging - synaptogenesis, gliogenesis and neurovascular coupling (see Lerch et al., 2017; Tardif et al., 2016; Zatorre et al., 2012 for discussion). Third, by including an identical fMRI task in the visual modality (see Supplementary Information 1.3) we showed that functional plasticity is specific to tactile reading and is not driven by a simple repetition effect. However, an appropriate control group will improve confidence in the specificity of the structural reorganization we observe in any repeat experiment.

A couple of perspectives for future research arise from our findings. Neuroplastic changes have been reported with training on a variety of time scales, ranging from minutes or hours to weeks and months (see Lövdén et al., 2013 for review). We report rapid functional reorganization of the reading network within the first weeks of training. How early the crucial adaptation processes occur needs an experimental design with multiple measurements during the first weeks of training. The exact role of myelin changes varies across cortical areas. Multiple reviews make claims that myelin fine-tunes local processing and provides the finishing touch to new circuit formation by regulating synaptic plasticity (Sampaio-Baptista and Johansen-Berg, 2017; Tardif et al., 2016). In this study, we focused on the various characteristics of grey matter. Myelin content is best studied in white matter with myelin sheath formation or remodelling mechanisms (Fields, 2015; Sampaio-Baptista and Johansen-Berg, 2017; Zatorre et al., 2012). Thus, tracing the time course of microstructural fibre reorganization may inform the process of neuroplasticity further. Previous studies exploring these issues suggest that changes will occur in the somatosensory (Debowska et al., 2016) and early visual cortex (Bola et al., 2017b). However, it is still unclear as to when such changes occur and whether they follow a similar time course to the grey matter reorganization we report.

## 5. Conclusions

In conclusion, by combining a longitudinal and multi-contrast MRI design, our study provides unique insight into the dynamics of neuroplasticity during human learning. We demonstrate that over the course of learning, functional reorganization precedes structural changes in grey matter. Our results show that while a developed reading network can rapidly adapt to stimuli conveyed in a novel modality, further neuroplastic changes are detected by anatomical changes in the relevant sensory cortices. Additionally, using a quantitative T1 mapping technique we show that previously neglected intracortical myelin plasticity plays a role in the reorganisation of reading-sensitive visual cortex during learning of a new script.

## Data availability statement

The source data used to create all figures (Fig. 2 - behavioural tests and accuracy in the fMRI task, Fig. 4 and 5 – region of interest data extracted from fMRI, GMV and R1 parameter, Fig. 6 - brain-behaviour correlations) as well as thresholded statistical maps from all whole brain group analysis are available in the Open Science Framework project: https://osf.io/hjy28/.

## Credit authorship contribution statement

**Jacek Matuszewski:** Methodology, Software, Validation, Formal analysis, Investigation, Resources, Data curation, Writing - original draft, Writing - review & editing, Visualization. **Bartosz Kossowski:** Methodology, Software, Validation, Formal analysis. **Łukasz Bola:** Methodology, Writing - review & editing. **Anna Banaszkiewicz:** Methodology, Investigation, Resources, Writing - review & editing. **Małgorzata Paplińska:** Methodology, Investigation, Resources. **Lucien Gyger:** Software, Validation, Formal analysis, Writing - review & editing. **Ferath Kherif:** Software, Formal analysis, Writing - review & editing. **Marcin Szwed:** Conceptualization, Methodology, Writing - review & editing. **Richard S. Frackowiak:** Methodology, Writing - review & editing. **Katarzyna Jednoróg:** Conceptualization, Methodology, Formal analysis, Writing - review & editing. **Bogdan Draganski:** Software, Methodology, Formal analysis, Writing - review & editing, Supervision. **Artur Marchewka:** Conceptualization, Methodology, Formal analysis, Resources, Writing - review & editing, Supervision, Project administration, Funding acquisition.

## Acknowledgments

The study was supported by the National Science Centre Poland grant (2014/14/M/HS6/00918) awarded to AM. JM was additionally supported by the National Science Centre Poland grant (2017/27/N/HS6/02669). The study was conducted with the aid of CePT research infrastructure purchased with funds from the European Regional Development Fund as part of the Innovative Economy Operational Programme, 2007–2013. BD is supported by the Swiss National Science Foundation (NCCR Synapsy, project grant Nr. 32003B_135679, 32003B_159780, 324730_192755 and CRSK-3_190185) and the Leenaards Foundation. LREN is very grateful to the Roger De Spoelberch and Partridge Foundations for their generous financial support.

## Declaration of Competing Interests

Authors declare no competing interests.

## Supplementary materials

Supplementary material associated with this article can be found, in the online version, at doi:10.1016/j.neuroimage.2020.117613.

## References

Amedi, A., Malach, R., Hendler, T., Peled, S., Zohary, E., 2001. Visuo-haptic object-related activation in the ventral visual pathway. Nat. Neurosci. 4, 324–330. https://doi.org/10.1038/85201.

Amedi, A., Stern, W.M., Camprodon, J.A., Bermpohl, F., Merabet, L., Rotman, S., Hemond, C., Meijer, P., Pascual-Leone, A., 2007. Shape conveyed by visual-to-auditory sensory substitution activates the lateral occipital complex. Nat. Neurosci. 10, 687–689. https://doi.org/10.1038/nn1912.

Amedi, A., Hofstetter, S., Maidenbaum, S., Heimler, B., 2017. Task-selectivity as a comprehensive principle for brain organization. Trends Cogn. Sci. 21 (5), 307–310. https://doi.org/10.1016/j.tics.2017.03.007.

Ashburner, J., 2007. A fast diffeomorphic image registration algorithm. Neuroimage 38, 95–113. https://doi.org/10.1016/j.neuroimage.2007.07.007.

Ashburner, J., Ridgway, G.R., 2013. Symmetric diffeomorphic modeling of longitudinal structural MRI. Front. Neurosci.. https://doi.org/10.3389/fnins.2012.00197.

Bakdash, J.Z., Marusich, L.R., 2017. Repeated measures correlation. Front. Psychol. 8, 456. doi:10.3389/fpsyg.2017.00456.

Banaszkiewicz, A, Matuszewski, J, Bola, Ł, Szczepanik, M., Kossowski, B., Rutkowski, P., Szwed, M., Emmorey, K., Jednoróg, K., Marchewka, A., 2020. Multimodal imaging of brain reorganization in hearing late learners of sign language. Hum Brain Mapp.. in press https://doi.org/10.1002/hbm.25229 .

Bedny, M., Pascual-Leone, A., Dodell-Feder, D., Fedorenko, E., Saxe, R., 2011. Language processing in the occipital cortex of congenitally blind adults. Proc. Natl. Acad. Sci. U. S. A. 108, 4429–4434. https://doi.org/10.1073/pnas.1014818108.

Bengtsson, S.L., Nagy, Z., Skare, S., Forsman, L., Forssberg, H., Ullén, F., 2005. Extensive piano practicing has regionally specific effects on white matter development. Nat. Neurosci. 8, 1148–1150. https://doi.org/10.1038/nn1516.

Bock, N.A., Kocharyan, A., Liu, J.V., Silva, A.C., 2009. Visualizing the entire cortical myelination pattern in marmosets with magnetic resonance imaging. J. Neurosci. Methods 185, 15–22. https://doi.org/10.1016/j.jneumeth.2009.08.022.

Bola, Ł., Matuszewski, J., Szczepanik, M., Droździel, D., Sliwinska, M.W., Paplińska, M., Jednoróg, K., Szwed, M., Marchewka, A., 2019. Functional hierarchy for tactile processing in the visual cortex of sighted adults. Neuroimage 202, 116084. https://doi.org/10.1016/j.neuroimage.2019.116084.

Bola, Ł., Radziun, D., Siuda-Krzywicka, K., Sowa, J.E., Paplinska, M., Sumera, E., Szwed, M., 2017a. Universal visual features might be necessary for fluent reading. a longitudinal study of visual reading in Braille and Cyrillic alphabets. Front. Psychol. 8. https://doi.org/10.3389/fpsyg.2017.00514.

Bola, Ł., Siuda-Krzywicka, K., Paplińska, M., Sumera, E., Hańczur, P., Szwed, M.S., 2016. Braille in the sighted: Teaching tactile reading to sighted adults. PLoS One 11. https://doi.org/10.1371/journal.pone.0155394.

Bola, Ł., Siuda-Krzywicka, K., Paplińska, M., Sumera, E., Zimmermann, M., Jednoróg, K., Marchewka, A., Szwed, M., 2017b. Structural reorganization of the early visual cortex following Braille training in sighted adults. Sci. Rep. 7. https://doi.org/10.1038/s41598-017-17738-8.

Brem, S., Bach, S., Kujala, J.V., Maurer, U., Lyytinen, H., Richardson, U., Brandeis, D., 2013. An electrophysiological study of print processing in kindergarten: the contribution of the visual n1 as a predictor of reading outcome. Dev. Neuropsychol. 38 (8), 567–594. https://doi.org/10.1080/87565641.2013.828729.

Büchel, C., Price, C., Frackowiak, R.S.J., Friston, K., 1998. Different activation patterns in the visual cortex of late and congenitally blind subjects. Brain 121, 409–419. https://doi.org/10.1093/brain/121.3.409.

Burton, H., Diamond, J.B., McDermott, K.B., 2003. Dissociating cortical regions activated by semantic and phonological tasks: A fMRI study in blind and sighted people. J. Neurophysiol. 90, 1965–1982. https://doi.org/10.1152/jn.00279.2003.

Callaghan, M.F., Helms, G., Lutti, A., Mohammadi, S., Weiskopf, N., 2015. A general linear relaxometry model of R1 using imaging data. Magn. Reson. Med. 73, 1309–1314. https://doi.org/10.1002/mrm.25210.

Carey, D., Caprini, F., Allen, M., Lutti, A., Weiskopf, N., Rees, G., Callaghan, M.F., Dick, F., 2018. Quantitative MRI provides markers of intra-, inter-regional, and age-related differences in young adult cortical microstructure. Neuroimage 182, 429–440. https://doi.org/10.1016/j.neuroimage.2017.11.066.

Cecchetti, L., Kupers, R., Ptito, M., Pietrini, P., Ricciardi, E., 2016. Are supramodality and cross-modal plasticity the yin and yang of brain development? from blindness to rehabilitation. Front. Syst. Neurosci. 10, 1–8. https://doi.org/10.3389/fnsys.2016.00089.

Chen, G., Adleman, N.E., Saad, Z.S., Leibenluft, E., Cox, R., 2014. Applications of multivariate modeling to neuroimaging group analysis: a comprehensive alternative to univariate general linear model. Neuroimage 99, 571–588. https://doi.org/10.1016/j.neuroimage.2014.06.027.

Chen, M.S., Huber, A.B., Van Der Haar, M.E.D., Frank, M., Schnell, L., Spillmann, A.A., …, Schwab, M.E., 2000. Nogo-A is a myelin-associated neurite outgrowth inhibitor and an antigen for monoclonal antibody IN-1. Nature 403 (6768), 434–439. https://doi.org/10.1038/35000219.

Collins, C.E., Airey, D.C., Young, N.A., Leitch, D.B., Kaas, J.H., 2010. Neuron densities vary across and within cortical areas in primates. Proceed. Natl. Acad. Sci. U. S. A. 107 (36), 15927–15932. https://doi.org/10.1073/pnas.1010356107.

Cousineau, D., 2005. Confidence intervals in within-subject designs: a simpler solution to Loftus and Masson's method. Tutor. Quant. Methods Psychol. 1, 42–45.

Debowska, W., Wolak, T., Nowicka, A., Kozak, A., Szwed, M., Kossut, M., 2016. Functional and structural neuroplasticity induced by short-term tactile training based on braille reading. Front. Neurosci. 10, 1–13. https://doi.org/10.3389/fnins.2016.00460.

Debowska, W., Wolak, T., Soluch, P., Orzechowski, M., Kossut, M., 2013. Design and evaluation of an innovative MRI-compatible Braille stimulator with high spatial and temporal resolution. J. Neurosci. Methods 213, 32–38. https://doi.org/10.1016/j.jneumeth.2012.12.002.

Dehaene, S., 2009. Reading in the brain: The new science of how we read. Penguin.

Dehaene, S., Cohen, L., 2011. The unique role of the visual word form area in reading. Trends Cogn. Sci. 15, 254–262. https://doi.org/10.1016/j.tics.2011.04.003.

Draganski, B., Ashburner, J., Hutton, C., Kherif, F., Frackowiak, R.S.J., Helms, G., Weiskopf, N., 2011. Regional specificity of MRI contrast parameter changes in normal ageing revealed by voxel-based quantification (VBQ). Neuroimage 55, 1423–1434. https://doi.org/10.1016/j.neuroimage.2011.01.052.

Draganski, B., Gaser, C., Busch, V., Schuierer, G., Bogdahn, U., May, A., 2004. Changes in grey, matter induced by training. Nature 427, 311–312. https://doi.org/10.1038/427311a.

Draganski, B., Kherif, F., Lutti, A., 2014. Computational anatomy for studying use-dependant brain plasticity. Front. Hum. Neurosci. 8. https://doi.org/10.3389/fnhum.2014.00380.

Eickhoff, S.B., Stephan, K.E., Mohlberg, H., Grefkes, C., Fink, G.R., Amunts, K., Zilles, K., 2005. A new SPM toolbox for combining probabilistic cytoarchitectonic maps and functional imaging data. Neuroimage 25, 1325–1335. https://doi.org/10.1016/j.neuroimage.2004.12.034.

Engvig, A., Fjell, A.M., Westlye, L.T., Moberget, T., Sundseth, O., Larsen, V.A., Walhovd, K.B., 2010. Effects of memory training on cortical thickness in the elderly. Neuroimage 52, 1667–1676. https://doi.org/10.1016/j.neuroimage.2010.05.041.

Fields, R.D., 2015. A new mechanism of nervous system plasticity: activity-dependent myelination. Nat. Rev. Neurosci. 16, 756–767. https://doi.org/10.1038/nrn4023.

Fischl, B., Dale, A.M., 1999. Measuring the thickness of the human cerebral cortex. NeuroImage.

Fox, J., 2015. Applied Regression Analysis and Generalized Linear Models. SAGE Publications Inc. SAGE Publications.

Freeman, S.A., Desmazières, A., Fricker, D., Lubetzki, C., Sol-Foulon, N., 2016. Mechanisms of sodium channel clustering and its influence on axonal impulse conduction. Cel. Mol. Life Sci. 73, 723–735. https://doi.org/10.1007/s00018-015-2081-1.

Glasser, M.F., Goyal, M.S., Preuss, T.M., Raichle, M.E., Van Essen, D.C., 2014. Trends and properties of human cerebral cortex: correlations with cortical myelin content. Neuroimage.. https://doi.org/10.1016/j.neuroimage.2013.03.060.

Glasser, M.F., van Essen, D.C., 2011. Mapping human cortical areas in vivo based on myelin content as revealed by T1- and T2-weighted MRI. J. Neurosci. 31 (32), 11597–11616. https://doi.org/10.1523/JNEUROSCI.2180-11.2011.

Gomez, J., Barnett, M.A., Natu, V., Mezer, A., Palomero-Gallagher, N., Weiner, K.S., Amunts, K., Zilles, K., Grill-Spector, K., 2017. Microstructural proliferation in human cortex is coupled with the development of face processing. Science (80) 355. https://doi.org/10.1126/science.aag0311.

Grydeland, H., Walhovd, K.B., Tamnes, C.K., Westlye, L.T., Fjell, A.M., 2013. Intracortical myelin links with performance variability across the human lifespan: results from T1- and T2- weighted MRI myelin mapping and diffusion tensor imaging. J. Neurosci. 33, 18618–18630. https://doi.org/10.1523/JNEUROSCI.2811-13.2013.

Haier, R.J., Karama, S., Leyba, L., Jung, R.E., 2009. MRI assessment of cortical thickness and functional activity changes in adolescent girls following three months of practice on a visual-spatial task. BMC Res. Notes 2 (174). https://doi.org/10.1186/1756-0500-2-174.

Heath, F., Hurley, S.A., Johansen-Berg, H., Sampaio-Baptista, C., 2017. Advances in Noninvasive Myelin Imaging. Dev. Neurobiol. Publ. Wiley Period. Inc. Dev. Neurobiol 78, 136–151. https://doi.org/10.1002/dneu.22552.

Helms, G., Dathe, H., Dechent, P., 2008. Quantitative FLASH MRI at 3T using a rational approximation of the Ernst equation. Magn. Reson. Med. 59, 667–672. https://doi.org/10.1002/mrm.21542.

Herholz, S.C., Zatorre, R.J., 2012. Musical training as a framework for brain plasticity: behavior, function, and structure. Neuron.. https://doi.org/10.1016/j.neuron.2012.10.011.

Hofstetter, S., Tavor, I., Moryosef, S.T., Assaf, Y., 2013. Short-term learning induces white matter plasticity in the fornix. J. Neurosci. 33, 12844–12850. https://doi.org/10.1523/JNEUROSCI.4520-12.2013.

Ilg, R., Wohlschläger, A.M., Gaser, C., Liebau, Y., Dauner, R., Wöller, A., …, Mühlau, M., 2008. Gray matter increase induced by practice correlates with task-specific activation: a combined functional and morphometric magnetic resonance imaging study. J. Neurosci. 28 (16), 4210–4215. https://doi.org/10.1523/JNEUROSCI.5722-07.2008.

Kaller, M.S., Lazari, A., Blanco-Duque, C., Sampaio-Baptista, C., Johansen-Berg, H., 2017. Myelin plasticity and behaviour — connecting the dots. Curr. Opin. Neurobiol. 47, 86–92. https://doi.org/10.1016/j.conb.2017.09.014.

Klinge, C., Eippert, F., Röder, B., Büchel, C., 2010. Corticocortical connections mediate primary visual cortex responses to auditory stimulation in the blind. J. Neurosci. 30, 12798–12805. https://doi.org/10.1523/JNEUROSCI.2384-10.2010.

Kolasinski, J., Makin, T.R., Jbabdi, S., Clare, X.S., Stagg, C.J., Johansen-Berg, H., 2016. Investigating the stability of fine-grain digit somatotopy in individual human participants. https://doi.org/10.1523/JNEUROSCI.1742-15.2016

Kuper, C., Matuszewski, J., Banaszkiewicz, A., Bola, Ł., Szczepanik, M., Draps, M., Kordos, P., Szwed, M., Jednoróg, K., Marchewka, A., 2020. Functional reorganization of the reading network in the course of foreign language acquisition. NeuroImage 226, 117544. https://doi.org/10.1016/j.neuroimage.2020.117544.

Kupers, R., Fumal, A., De Noordhout, A.M., Gjedde, A., Schoenen, J., Ptito, M., 2006. Transcranial magnetic stimulation of the visual cortex induces somatotopically organized qualia in blind subjects. Proc. Natl Acad. Sci. USA 103, 13256–13260. https://doi.org/10.1073/pnas.0602925103.

Kwok, V., Niu, Z., Kay, P., Zhou, K., Mo, L., Jin, Z., So, K.F., Tan, L.H., 2011. Learning new color names produces rapid increase in gray matter in the intact adult human cortex. Proc. Natl. Acad. Sci. U. S. A. 108, 6686–6688. https://doi.org/10.1073/pnas.1103217108.

Lerch, J.P., Yiu, A.P., Martinez-Canabal, A., Pekar, T., Bohbot, V.D., Frankland, P.W., …, Sled, J.G., 2011. Maze training in mice induces MRI-detectable brain shape changes specific to the type of learning. NeuroImage 54 (3), 2086–2095. https://doi.org/10.1016/j.neuroimage.2010.09.086.

Lerch, J.P., Van Der Kouwe, A.J.W., Raznahan, A., Paus, T., Johansen-Berg, H., Miller, K.L., Smith, S.M., Fischl, B., Stamatios, &, 2017. Studying neuroanatomy using MRI 20. https://doi.org/10.1038/nn.4501

Lerma-Usabiaga, G., Carreiras, M., Paz-Alonso, P.M., 2018. Converging evidence for functional and structural segregation within the left ventral occipitotemporal cortex in reading. Proc. Natl. Acad. Sci. U. S. A. 115, E9981–E9990. https://doi.org/10.1073/pnas.1803003115.

Li, P., Legault, J., Litcofsky, K.A., 2014. Neuroplasticity as a function of second language learning: Anatomical changes in the human brain. Cortex 58, 301–324. https://doi.org/10.1016/j.cortex.2014.05.001.

Lorio, S., Fresard, S., Adaszewski, S., Kherif, F., Chowdhury, R., Frackowiak, R.S., Ashburner, J., Helms, G., Weiskopf, N., Lutti, A., Draganski, B., 2016. New tissue priors for improved automated classification of subcortical brain structures on MRI. Neuroimage 130, 157–166. https://doi.org/10.1016/j.neuroimage.2016.01.062.

Lövdén, M., Bäckman, L., Lindenberger, U., Schaefer, S., Schmiedek, F., 2010. A theoretical framework for the study of adult cognitive plasticity. Psychol. Bull. 136 (4), 659–676. https://doi.org/10.1037/a0020080.

Lövdén, M., Wenger, E., Mårtensson, J., Lindenberger, U., Bäckman, L., 2013. Structural brain plasticity in adult learning and development. Neurosci. Biobehav. Rev. 37, 2296–2310. https://doi.org/10.1016/j.neubiorev.2013.02.014.

Lutti, A., Dick, F., Sereno, M.I., Weiskopf, N., 2014. Using high-resolution quantitative mapping of R1 as an index of cortical myelination. Neuroimage 93, 176–188. https://doi.org/10.1016/j.neuroimage.2013.06.005.

Mandera, P., Keuleers, E., Wodniecka, Z., Brysbaert, M., 2014. Subtlex-pl: subtitle-based word frequency estimates for Polish. Behav. Res. Methods 47, 471–483. https://doi.org/10.3758/s13428-014-0489-4.

Maurer, U., Brem, S., Bucher, K., Kranz, F., Benz, R., Steinhausen, H.C., Brandeis, D., 2007. Impaired tuning of a fast occipito-temporal response for print in dyslexic children learning to read. Brain 130, 3200–3210. https://doi.org/10.1093/brain/awm193.

Maurer, U., Schulz, E., Brem, S., van der Mark, S., Bucher, K., Martin, E., Brandeis, D., 2011. The development of print tuning in children with dyslexia: evidence from longitudinal ERP data supported by fMRI. NeuroImage vol 57, 714–722. https://doi.org/10.1016/j.neuroimage.2010.10.055.

Mcfarquhar, M., Mckie, S., Emsley, R., Suckling, J., Elliott, R., Williams, S., 2016. Multivariate and repeated measures (MRM): A new toolbox for dependent and multimodal group-level neuroimaging data. https://doi.org/10.1016/j.neuroimage.2016.02.053

McGee, A.W., Strittmatter, S.M., 2003. The Nogo-66 receptor: focusing myelin inhibition of axon regeneration. Trends in Neurosciences 26 (4), 193–198. https://doi.org/10.1016/S0166-2236(03)00062-6.

McGee, A.W., Yang, Y., Fischer, Q.S., Daw, N.W., Strittmatter, S.H., 2005. Experience-driven plasticity of visual cortex limited by myelin and nogo receptor. Science 309 (5744), 2222–2226. https://doi.org/10.1126/science.1114362.

Merabet, L.B., Hamilton, R., Schlaug, G., Swisher, J.D., Kiriakopoulos, E.T., Pitskel, N.B., Kauffman, T., Pascual-Leone, A., 2008. Rapid and reversible recruitment of early visual cortex for touch. PLoS One 3. https://doi.org/10.1371/journal.pone.0003046.

Müller, Franziska, Niso, Guiomar, Samiee, Soheila, Ptito, Maurice, Baillet, Sylvain, Kupers, Ron, 2019. A thalamocortical pathway for fast rerouting of tactile information to occipital cortex in congenital blindness. Nature Communications 10. doi:10.1038/s41467-019-13173-7, 5154 (2019).

Natu, V.S., Gomez, J., Barnett, M., Jeska, B., Kirilina, E., Jaeger, C., Zhen, Z., Cox, S., Weiner, K.S., Weiskopf, N., Grill-Spector, K., 2019. Apparent thinning of human visual cortex during childhood is associated with myelination. Proc. Natl. Acad. Sci. U. S. A. 116, 20750–20759. https://doi.org/10.1073/pnas.1904931116.

Négyessy, L., Nepusz, T., Kocsis, L., Bazsó, F., 2006. Prediction of the main cortical areas and connections involved in the tactile function of the visual cortex by network analysis. Eur. J. Neurosci. 23, 1919–1930. https://doi.org/10.1111/j.1460-9568.2006.04678.x.

Pascual-Leone, A., Hamilton, R., 2001. The metamodal organization of the brain. Progr. Brain Res. 134, 427–445. https://doi.org/10.1016/S0079-6123(01)34028-1.

Pattamadilok, C., Planton, S., Bonnard, M., 2019. Spoken language coding neurons in the visual word form area: evidence from a TMS adaptation paradigm. NeuroImage 186, 278–285. https://doi.org/10.1016/j.neuroimage.2018.11.014.

Preibisch, C., Deichmann, R., 2009. Influence of RF spoiling on the stability and accuracy of T1 mapping based on spoiled FLASH with varying flip angles. Magn. Reson. Med. 61, 125–135. https://doi.org/10.1002/mrm.21776.

Price, C.J., Devlin, J.T., 2011. The interactive account of ventral occipitotemporal contributions to reading. Trends Cogn. Sci. 15, 246–253. https://doi.org/10.1016/j.tics.2011.04.001.

Ptito, M., Moesgaard, S., Gjedde, A., Kupers, R., 2005. Cross-modal plasticity revealed by electrotactile stimulation of the tongue in the congenitally blind. Brain 128, 606–614. https://doi.org/10.1093/brain/awh380.

R Core Team (2020). R: A language and environment for statistical computing. R Foundation for Statistical Computing, Vienna, Austria. https://www.R-project.org/.

Reich, L., Szwed, M., Cohen, L., Amedi, A., 2011. A ventral visual stream reading center independent of visual experience. Curr. Biol. 21, 363–368. https://doi.org/10.1016/j.cub.2011.01.040.

Ridgway, G.R., Omar, R., Ourselin, S., Hill, D.L.G., Warren, J.D., Fox, N.C., 2009. Issues with threshold masking in voxel-based morphometry of atrophied brains. Neuroimage 44, 99–111. https://doi.org/10.1016/j.neuroimage.2008.08.045.

Sadato, N., Okada, T., Honda, M., Yonekura, Y., 2002. Critical period for cross-modal plasticity in blind humans: a functional MRI study. Neuroimage 16, 389–400. https://doi.org/10.1006/nimg.2002.1111.

Sadato, N., Pascual-Leone, A., Grafman, J., Ibañez, V., Deiber, M.P., Dold, G., Hallett, M., 1996. Activation of the primary visual cortex by Braille reading in blind subjects. Nature.. https://doi.org/10.1038/380526a0.

Saito, D.N., Okada, T., Honda, M., Yonekura, Y., Sadato, N., 2006. Practice makes perfect: The neural substrates of tactile discrimination by Mah-Jong experts include the primary visual cortex. BMC Neurosci 7, 79. https://doi.org/10.1186/1471-2202-7-79.

Sampaio-Baptista, C., Johansen-Berg, H., 2017. White matter plasticity in the adult brain. Neuron 96, 1239–1251. https://doi.org/10.1016/j.neuron.2017.11.026.

Sampaio-Baptista, C., Khrapitchev, A.A., Foxley, S., Schlagheck, T., Scholz, J., Jbabdi, S., DeLuca, G.C., Miller, K.L., Taylor, A., Thomas, N., Kleim, J., Sibson, N.R., Bannerman, D., Johansen-Berg, H., 2013. Motor skill learning induces changes in white matter microstructure and myelination. J. Neurosci. 33, 19499–19503. https://doi.org/10.1523/JNEUROSCI.3048-13.2013.

Schmidt-Wilcke, T., Rosengarth, K., Luerding, R., Bogdahn, U., Greenlee, M.W., 2010. Distinct patterns of functional and structural neuroplasticity associated with learning Morse code. Neuroimage 51, 1234–1241. https://doi.org/10.1016/j.neuroimage.2010.03.042.

Schmidt-Wilcke, T., Wulms, N., Heba, S., Pleger, B., Puts, N.A., Glaubitz, B., Kalisch, T., Tegenthoff, M., Dinse, H.R., 2018. Structural changes in brain morphology induced by brief periods of repetitive sensory stimulation. Neuroimage 165, 148–157. https://doi.org/10.1016/j.neuroimage.2017.10.016.

Scholz, J., Klein, M.C., Behrens, T.E.J., Johansen-Berg, H., 2009. Training induces changes in white-matter architecture. Nat. Neurosci. 12, 1370–1371. https://doi.org/10.1038/nn.2412.

Sereno, M.I., Lutti, A., Weiskopf, N., Dick, F., 2013. Mapping the Human Cortical Surface by Combining Quantitative T1 with Retinotopy†. Cereb. Cortex 23, 2261–2268. https://doi.org/10.1093/cercor/bhs213.

Siuda-Krzywicka, K., Bola, Ł., Paplińska, M., Sumera, E., Jednoróg, K., Marchewka, A., Śliwińska, M.W., Amedi, A., Szwed, M., 2016. Massive cortical reorganization in sighted braille readers. Elife 5, 1–26. https://doi.org/10.7554/eLife.10762.

Stüber, C., Morawski, M., Schäfer, A., Labadie, C., Wähnert, M., Leuze, C., Streicher, M., Barapatre, N., Reimann, K., Geyer, S., Spemann, D., Turner, R., 2014. Myelin and iron concentration in the human brain: A quantitative study of MRI contrast. Neuroimage 93, 95–106. https://doi.org/10.1016/j.neuroimage.2014.02.026.

Tabelow, K., Balteau, E., Ashburner, J., Callaghan, M.F., Draganski, B., Helms, G., Kherif, F., Leutritz, T., Lutti, A., Phillips, C., Reimer, E., Ruthotto, L., Seif, M., Weiskopf, N., Ziegler, G., Mohammadi, S., 2019. hMRI – A toolbox for quantitative MRI in neuroscience and clinical research. Neuroimage.. https://doi.org/10.1016/j.neuroimage.2019.01.029.

Tardif, C.L., Gauthier, C.J., Steele, C.J., Bazin, P.-L., Schäfer, A., Schaefer, A., Turner, R., Villringer, A., 2016. Advanced MRI techniques to improve our understanding of experience-induced neuroplasticity. https://doi.org/10.1016/j.neuroimage.2015.08.047

Weiskopf, N., Mohammadi, S., Lutti, A., Callaghan, M.F., 2015. Advances in MRI-based computational neuroanatomy: from morphometry to in-vivo histology. Curr. Opin. Neurol. 28, 313–322. https://doi.org/10.1097/WCO.0000000000000222.

Wenger, E., Brozzoli, C., Lindenberger, U., Lövdén, M., 2017. Expansion and renormalization of human brain structure during skill acquisition. Trends Cogn. Sci.. https://doi.org/10.1016/j.tics.2017.09.008.

Wittenberg, G.F., Werhahn, K.J., Wassermann, E.M., Herscovitch, P., Cohen, L.G., 2004. Functional connectivity between somatosensory and visual cortex in early blind humans. Eur. J. Neurosci. 20, 1923–1927. https://doi.org/10.1111/j.1460-9568.2004.03630.x.

Zangaladze, A., Epstein, C.M., Grafton, S.T., Sathian, K., 1999. Involvement of visual cortex in tactile discrimination of orientation. Nature 401, 587–590. https://doi.org/10.1038/44139.

Zatorre, R.J., Fields, R.D., Johansen-Berg, H., 2012. Plasticity in gray and white: Neuroimaging changes in brain structure during learning. Nat. Neurosci. 15, 528–536. https://doi.org/10.1038/nn.3045.